An integrated High-Pressure, Pressure Temperature and Skin Friction Sensor

Alexander K Sang and Clark Boyd

Luna Innovations Incorporated, 3157 State St., Blacksburg, VA 24060.

ABSTRACT

We present a prototype fiber-optic temperature, pressure and skin friction sensor suite for possible use in a deep water petroleum pipeline containing corrosive, multi-phase flow with solid particulates in a pressure and temperature gradient. The sensor suite is designed to measure shear stress ranging from 0-1,000 Pa, temperature from 0-175 Deg C and pressure from 5-69MPa. Each transducer was individually tested over the entire performance range. The integrated sensor package was tested over a limited temperature, pressure and shear range due to facility limitations.

Keywords: temperature, pressure, fiber-optic, EFPI, skin friction, downhole, shear stress

1. INTRODUCTION

The use of optical fibers as a sensing mechanism has proven to be useful in the oil and gas industry due to desirable electrical and mechanical characteristics which include EMI immunity, small size and light weight. This is particularly necessary in offshore sites where pipelines may cover tens of kilometers on the sea floor at depths greater than three kilometers carrying potentially corrosive, multi-phase product at high temperature and pressure. In order to ensure safe, efficient transport and optimal production of the fluid, near real-time monitoring of the fluid is critical.

In this paper, we present a prototype sensor suite for flow characterization and parameter monitoring. The non-intrusive sensor package directly measures flow shear, temperature and pressure.

2. THEORY OF OPERATION

The transducing mechanism used by all the sensors described herein utilize Extrinsic Fabry-Perot Interferometry (EFPI), a distance measurement technique based on the formation of a low-finesse Fabry-Perot cavity between the polished end face of an optical fiber and a reflective surface, shown schematically in figure 1 below[1,2]. Light is emitted from a broadband source, transmitted through a coupler, and passed through the fiber at the sensor, where a portion of the light is reflected off the fiber end face (R_1). The remaining light propagates through the gap and is reflected back into the fiber (R_2). R_1 is the reference reflection while R_2 is the sensing reflection. In a pressure sensor, R_1 is formed at the fiber/air interface while R_2 may be formed on the reflective pressure-sensitive diaphragm. For a temperature sensor, R_1 is formed at the fiber/sensor chip interface while R_2 is formed at the polished face of the sensor chip. These two light waves interfere constructively or destructively based on the path length difference traversed by the sensing reflection relative to the reference reflection and travel back through the single mode fiber to the demodulation unit. The resulting interference pattern is then interpreted, and the absolute gap (optical path length) between the two reflectors is calculated. The physical quantity measured is the optical path length between R_1 and R_2.

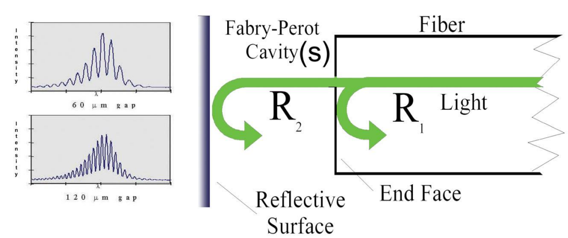

Figure 1. EFPI concept illustration

The optical return from an EFPI sensor can be modeled by[3]:

$$I = \left|\overline{U}_1 + \overline{U}_2\right|^2 = A_1^{\,2} + A_2^{\,2} + 2A_1A_2\cos(\phi_1 - \phi_2) \tag{1}$$

Fiber Optic Sensors and Applications VI, edited by Eric Udd, Henry H. Du, Anbo Wang, Proc. of SPIE Vol. 7316, 731613
© 2009 SPIE · CCC code: 0277-786X/09/$18 · doi: 10.1117/12.820818

where "I" is the optical power return from the sensor, A_1^2 and A_2^2 are the complex amplitudes of reflections R_1 and R_2 and $\phi_1 - \phi_2 = \Delta\phi$ is the difference in phase of the two reflections.

3. SKIN FRICTION SENSOR

The skin friction sensor used in this study is a non-intrusive, direct measuring concept. A floating element on a beam or flexure, flush to the bounding surface measures the shear applied by the moving fluid. As a consequence, no prior knowledge of the flow is necessary. The flexure is designed to have axial stiffness, to minimize normal pressure effects while being weak to tangential forces, thus increasing instrument sensitivity to shear. The deflection of the floating element is calibrated to correspond with the applied shear stress. This concept is illustrated in figure 2a.

In this sensor, the EFPI gap was formed by the fiber end face and the polished surface of the floating element as illustrated in figure 2b.

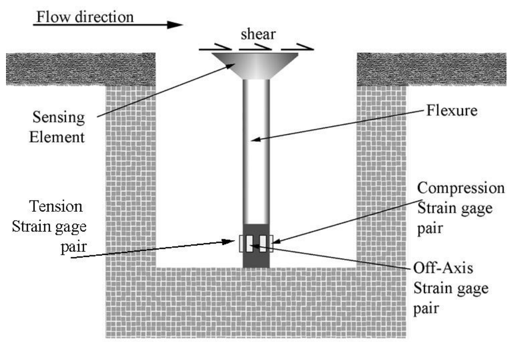

a) A basic Non-nulling beam

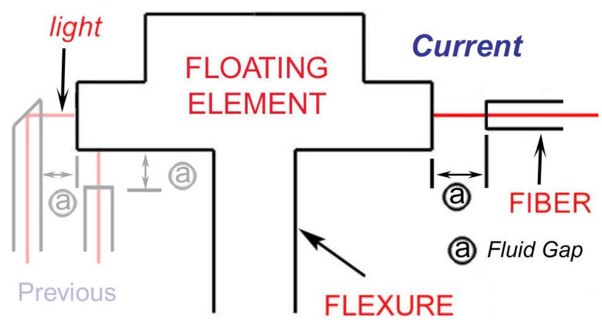

b) Gap Interrogation concept

Figure 2 Skin friction sensor concept and measuring technique

In order to meet the specified design pressure operating requirements, a low compressibility fluid was used to fill the sensor internal volume. A bellows was integrated into the design to separate the production fluid from the sensor fill-fluid. The gap interrogation method selected was a side-viewing straight cleaved fiber, combination of the previously studied techniques (see figure 2b). This combination resulted in improved sensor performance; however, the fiber could not be contained in the sensor volume in this prototype configuration. Figure 3 is an illustration of the final sensor assembly.

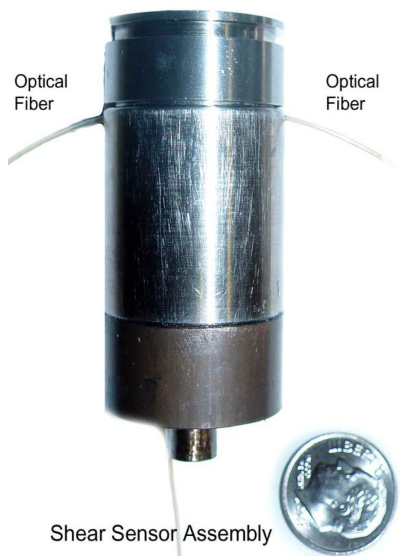

Figure 3. Shear sensor assembly

A. SENSOR CALIBRATION

A point load calibration method was used to correlate sensor deflection to shear. A known weight is placed parallel to the direction of flow and perpendicular to the sensing element. This is usually achieved by hanging a paper cone by sewing thread attached to the floating element with clear tape as illustrated in figure 4a. Different weights ranging from 50 milligrams to 10 grams are placed in the cone while the corresponding output is recorded. The gage is then rotated 180 degrees and the procedure repeated.

The mass calibration is then related to shear through Equation (1):

$$\tau_w = \frac{K * M}{A} \tag{1}$$

where **K** is the conversion factor from mass to force units, **M** is the mass of the calibration weight and **A** is sensing head area. A calibration curve can then be generated in the form of:

$$\tau_w = S * D + B \tag{2}$$

where **S** is the slope of the calibration curve, **D** is the measured deflection and **B** is the y-intercept, which is generally zero.

Sensor calibration was repeated multiple times to obtain a statistically significant data set for accurate sensor characterization. Figure 4b below is the Gap versus shear curve which has a 99.99% correlation to a linear fit. A slope of 221.9 Pa/Micron was obtained.

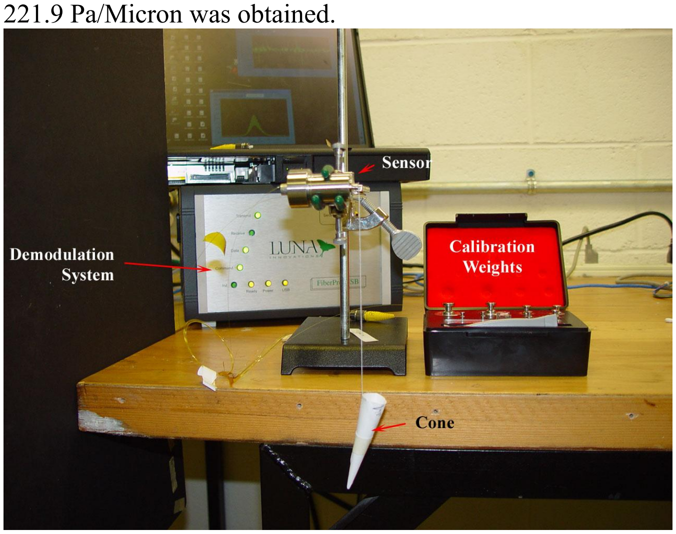

a) Calibration Setup of Shear Sensor

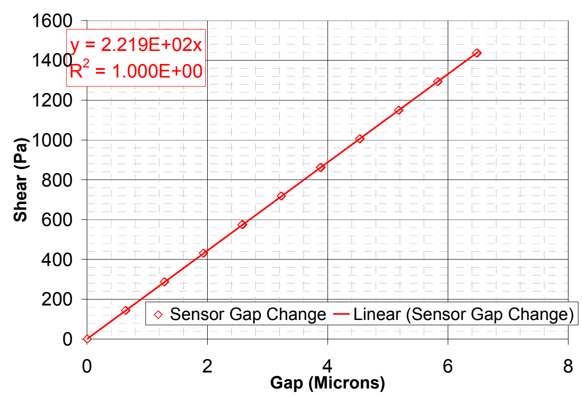

b) Shear Sensor Calibration Curve

Figure 4. Shear sensor calibration

B. TEMPERATURE COMPENSATION

Earlier studies revealed that the optically clear heat transfer oil used to fill the sensor internal volume showed that the fluid index of refraction varied linearly with temperature as illustrated in figure 5.

The measurement made using the EFPI technique is a product of the index of refraction and the actual gap, hence, an apparent change in gap would be detected with a corresponding temperature variation as illustrated in equation (3) below:

$$G_m = n(t) \times G_a \tag{3}$$

where G_m is the measure gap, *n(t)* is the index of refraction as a function of temperature and G_a is the actual gap. A fiber optic temperature transducer was used to monitor the gage internal temperature to account for index of refraction variation with temperature and thus enable thermal compensation. Figure 6 is an example of sensor gap test data with and without temperature compensation.

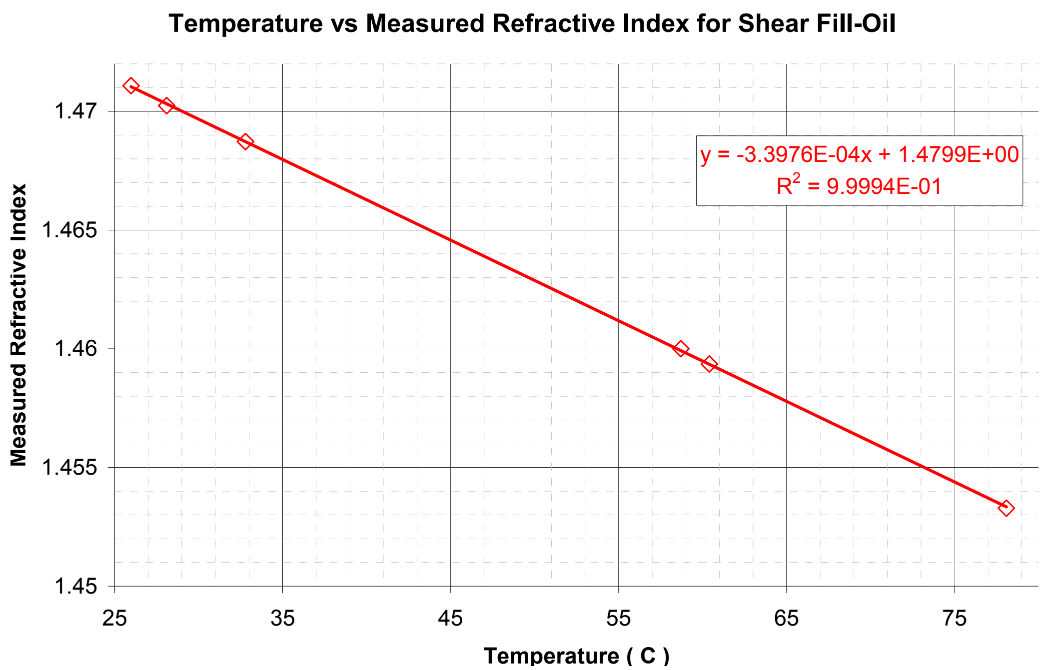

Figure 5. Index of refraction change as a function of temperature for sensor fill fluid

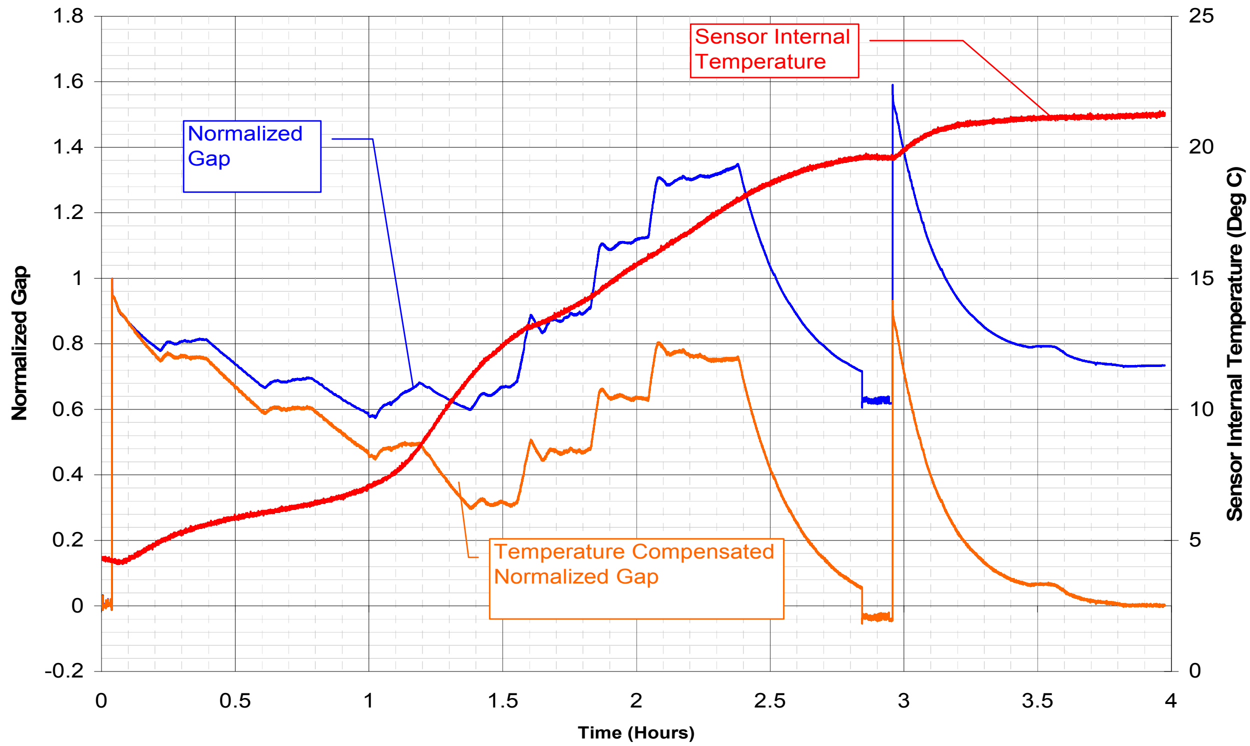

Figure 6. Illustration of temperature compensation on shear sensor measured gap

4. TEMPERATURE/PRESSURE SENSOR

The single-point fiber optic, temperature/pressure transducer core used in this investigation consists of a silica capillary tube fused to optical fiber as illustrated in figure 7a. A photograph of joint region of the prototype sensor is shown in 7b.

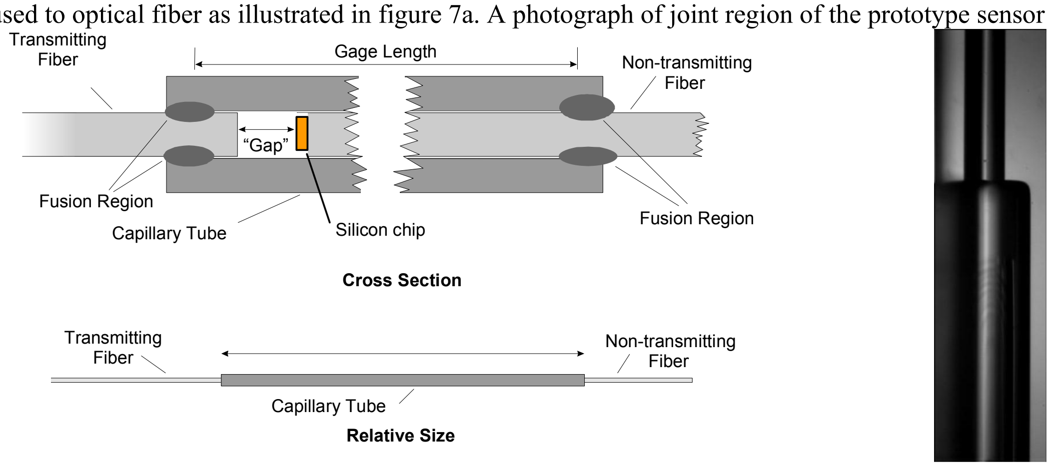

a) Fused EFPI sensing element *b) Sensor Bond Region*

Figure 7. Pressure/temperature core design concept

A pressure measurement is made by monitoring the gap between the transmitting fiber end face and the silicon chip. This gap decreases as a hydrostatic pressure is applied to the fiber element. Temperature measurement is done by monitoring the change in thickness of the silicon chip attached to non-transmitting fiber. The sensor core is isolated from the working fluid via a compliant metal diaphragm. The assembly is packaged into a rugged housing capable of withstanding extreme vibration and shock typically seen during sensor deployment.

C. SENSOR CALIBRATION

The Pressure/Temperature sensor assembly was calibrated using a high precision dead weight tester and an Environmental chamber. The calibration was performed by attaching high pressure tubing from the dead weight tester to the sensor assembly located inside the environmental chamber. The Environmental chamber then swept through the required temperature range, dwelling at specified, evenly spaced intervals. Once thermal equilibrium was attained at t at a specific temperature point, a pressure calibration was performed. This procedure was repeated until the entire temperature and pressure range was covered. Table 1 describes the temperature and pressure intervals used for sensor calibration.

Table 1.Temperature and Pressure Calibration Ranges

Parameter	**Lower Limit**	**Upper Limit**	**Interval**
Pressure (psi)	14.4	10,000	500
Temperature (^0C)	0	150	5

Figure 10 and 11 are the sensor gap changes due to the applied pressure and temperature. The data showed that the pressure gap changed with temperature. It was therefore necessary to correlate the pressure to both the temperature and pressure gap changes. This resulted in a dual-variable polynomial illustrated in equation (1) below:

$$P = a_0 + a_1 x + a_2 y + a_3 x^2 + a_4 xy + a_5 y^2 + a_6 x^3 + a_7 x^2 y + a_7 x^2 y + a_8 xy^2 + a_9 y^3 \quad (1)$$

Where **P** is the calculated pressure, **x** is the pressure sensor gap reading, **y** is the temperature sensor gap reading and $\mathbf{a_0}$-$\mathbf{a_9}$ are calibration coefficients. The data further showed that temperature gap was independent of pressure hence, led to a much simplified third order polynomial correlation as seen in equation (2) below:

$$T = b_0 + b_1 y + b_2 y^2 + b_3 y^3 \quad (2)$$

Where **T** is the calculated temperature and $\mathbf{b_0}$-$\mathbf{b_3}$ are the calibration coefficients.

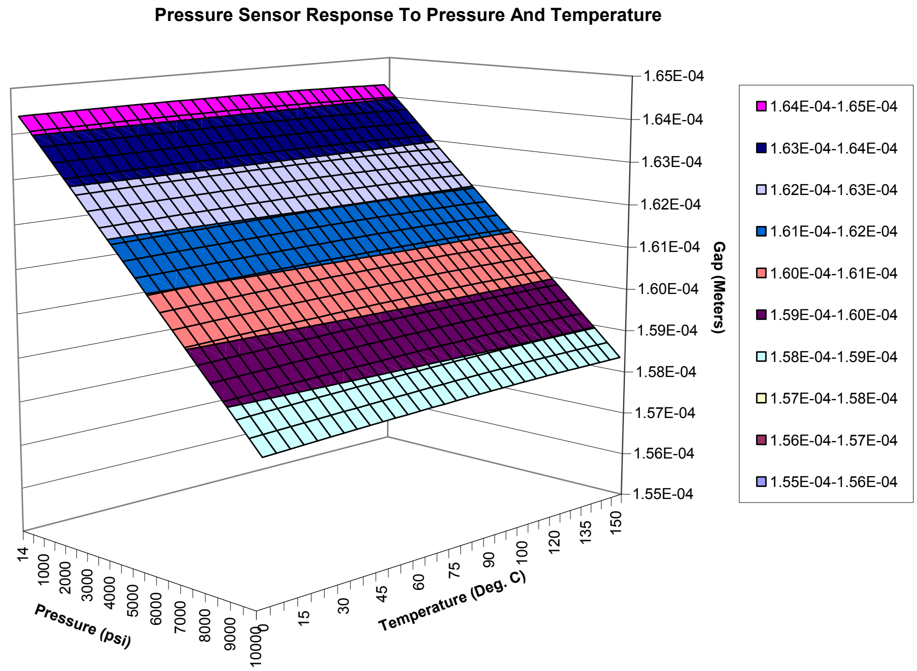

Figure 8. Pressure sensor calibration

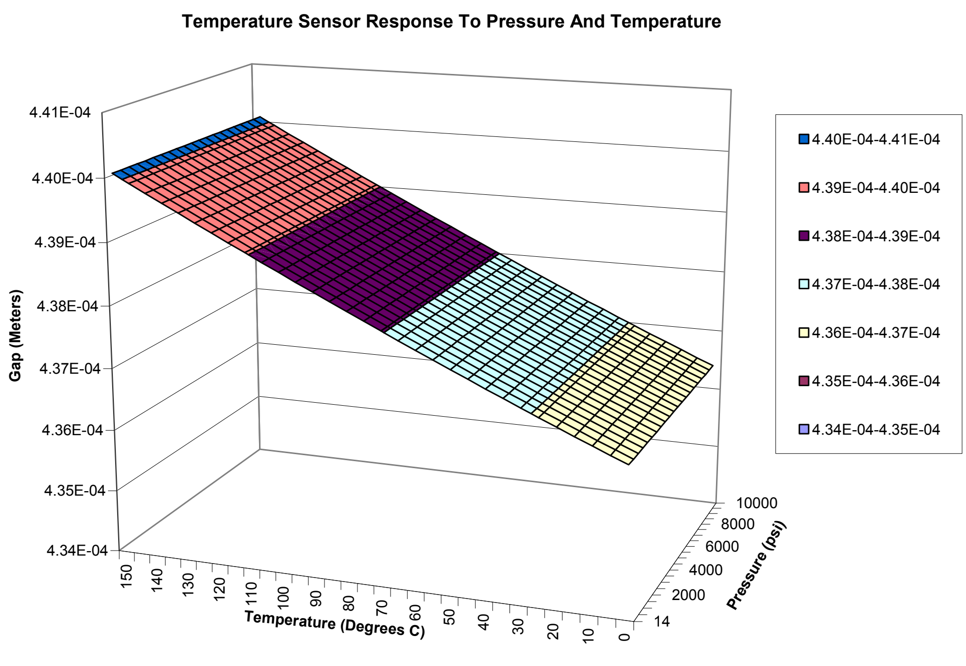

Figure 9. Temperature sensor calibration

5. CALIBRATION STATISTICS

Table 2 shows various statistical properties calculated from the Temperature/Pressure and Shear sensors showing sensor performance within the intended design specifications.

Table 2. Shear Sensor Statistical Properties

Statistical Property	Pressure Sensor (psi)	Temperature Sensor (^{0}C)	Shear Sensor (Pascal)
Mean	0.0067	-1.23E-05	-1.604
Standard Error	0.0890	0.0032	0.173
Median	0	-0.002	-1.533
Mode	-1	-0.005	-0.337
Standard Deviation	1.543	0.0809	1.405
Sample Variance	2.3811	0.0065	1.974
Kurtosis	-0.5617	0.1111	-0.617
Skewness	0.1922	-0.0813	0.004
Range	9	0.5	5.975
Sum	2	-0.008	-105.835
Count	300	651	66
Largest(1)	5	0.224	1.351
Smallest(1)	-4	-0.276	-4.623
Confidence Level (99.5%)	0.2520	0.0089	0.345
3σ	4.6294	0.2427	4.215
%FS	0.04630	0.1618	0.422%

6. TEST FACILITY

The sensor platform was tested in a custom built test facility designed to provide a distributed shear on skin friction gages using a synthetic grade glycerin flowing under fully-developed conditions in a two dimensional channel. The fully-developed condition refers to the situation where the boundary layer on the top and bottom surfaces of the channel grow and finally converge at the channel centerline, impeding further boundary layer development resulting in an identical mean flow velocity profile.

A tank 49 inches tall with a 12-inch diameter supplies glycerin to a 16 inch long and 1/4 inch high two-dimensional channel. The top surface of the 2-D channel is made of a hard plastic that has pressure portals equally spaced over the entire length of the channel. A flow valve located at the end of the channel controls the stream of glycerin. When the valve is open the glycerin flows into a collecting tank located below the channel opening. The tank and bottom portion of the flow channel is made of aluminum and has quarter inch channels through which heated or cooled fluid allowing for the alteration of the flow temperature. The operating principle of the calibration rig is based on equation (1):

$$\tau_w = -\frac{dp}{dx}h \tag{1}$$

where $\frac{dp}{dx}$ is the pressure gradient, and h is the channel height measured from the centerline. With the flow valve closed, the head pressure generated by the fluid in the glycerin tank is equally transmitted along the length of the channel. When the flow valve is opened, the pressure at the exit drops to room pressure, creating a pressure difference along the length of the channel. Measurement is done after the flow reaches steady state. Different shear values can be obtained by varying the fluid level in the glycerin tank. This results in a change in the pressure gradient represented in Equation (1) due to the alteration of the head pressure. A 1 Hp. pump is used to transfer glycerin from the collecting tank into the glycerin tank. The pump is fitted with a variable frequency drive that permits the adjustment of the fluid flow rate. This will enable variation of shear values imparted to the sensor assembly. Figure 10 is an image of the flow test facility.

Figure 10. Luna Innovations flow test facility

7. TEMPERATURE/PRESSURE/SHEAR SENSOR TESTING

A common housing was designed and fabricated to enable sensor testing in the Luna Innovations Flow facility. Figure 11 is an illustration of the assembled sensor.

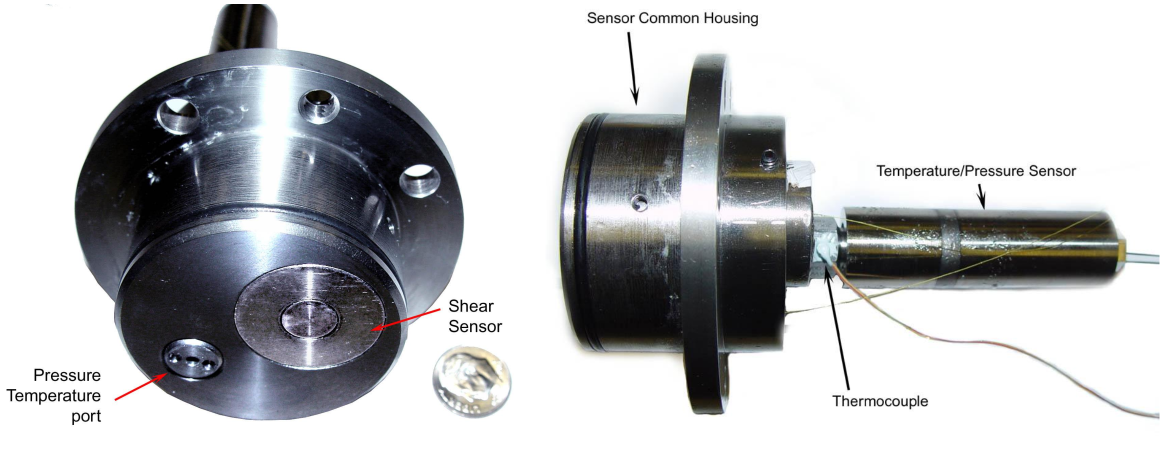

a) Front view *b) Side view*

Figure 11. Temperature/Pressure Shear Housing

Due to the limitations of the Flow test Facility, a limited range of temperature, pressure and shear was tested. Earlier investigations into expanding the test range of the facility proved to be cost prohibitive. Table 3 shows the test parameter limits investigated.

Table 3. Test Range Investigated for various Parameters

Test	Minimum	Maximum
Shear (Pa)	0	110
Temperature (^{0}C)	5	20
Pressure (psi$_g$)	0	2

A long duration test was designed to enable the variation of temperature, pressure and shear. The initial segment of the test involved a pressure test. The facility main tank was filled with glycerin with the front valve closed resulting in a 2 psi_g pressure increase. Figure 12 shows the Temperature/Pressure/Shear (TPS) sensor response to the applied static pressure.

The correlation of the measured TPS senor pressure to that of the test facility was non-linear during the transient portion of the test. The sensor does accurately resolve the pressure at steady state portion of the test. It is worth noting that all the data collected was within the designed accuracy of the sensor.
A temperature and Shear test was performed on the TPS sensor. To enable a temperature change, the facility was chilled to 4 degrees C. and allowed to gradually warm up during shear testing by turning off the system chiller. A thermocouple was located near the TPS temperature sensor to enable temperature correlation. Figure 13 and figure 14 shows the TPS sensor response to Temperature and shear.

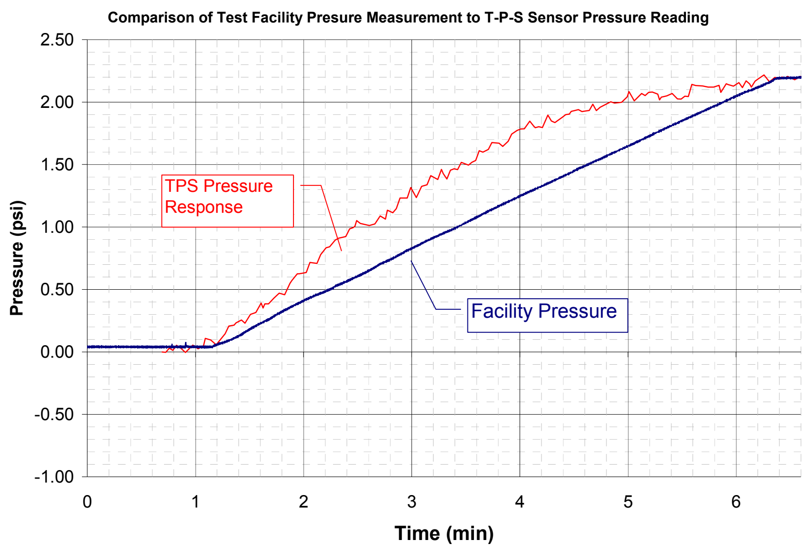

Figure 12. Comparison of TPS sensor and Test Facility pressure response

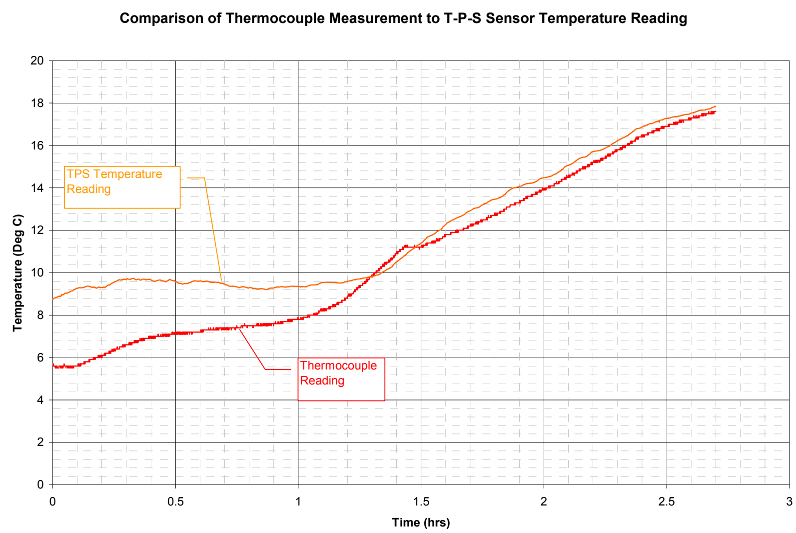

Figure 13. TPS sensor response to temperature

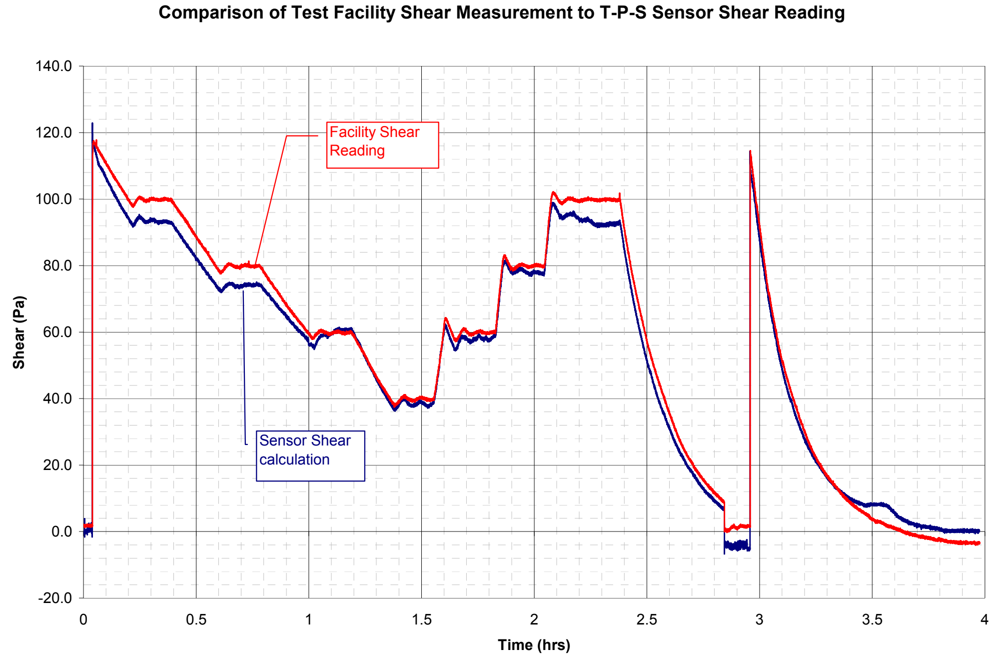

Figure 14. TPS sensor response to shear.

The temperature correlation between the thermocouple and the TPS sensor is good; however, improved correlation is attained at higher temperatures implying the influence of the surroundings on the TPS temperature reading.

For the shear test, the facility controlled to shear levels of 100, 80 60 and 40 Pa. The last portion of the test had shear continuously changing from 100 to 0 Pa. The shear reading correlated well through out the entire tests. Differences in the shear reading between the sensor and the calibration facility could be partially attributed to the facilty instrumentation drift. This is supported by the fact that the final shear reading of the TPS sensor was zero Pa whereas the facility reading was negative when the expected shear value was zero Pa.

8. Conclusion

Luna Innovations has successfully developed the technology for a temperature, pressure and shear sensor for application in sub sea pipelines. The sensors have been successfully integrated and tested over a limited segment of the operating range. Experiments demonstrated good sensor correlation over the tested range. Further proposed development will include the implementation of ruggedizing methods for the optics that will increase the life of the sensor.

9. Acknowledgments

Research and development on this project was funded in part by the National Institute of Standards and Technology under contract number 70NANB1H3064.

10. References

1. K. Murphy, M. Gunther, A. Vengsarkar, and R. Claus, "Quadrature phase-shifted, extrinsic Fabry-Perot optical fiber sensors", Optics Letters, Vol. 16, No. 4, February 1991, pp. 173-275.
2. Murphy, et. al., Extrinsic Fiber Optic Displacement Sensors and Displacement Sensing Systems, United States Patent #5,301,001.
3. T. Yoshino, K. Kurosawa, K. Itoh, and T. Ose, "Fiber-optic Fabry-Perot interferometer and its sensor applications," IEEE J. Quantum Electron., vol. QE-18, pp. 1624-1632, 1982.